JOURNAL OF THERMOPHYSICS AND HEAT TRANSFER
Vol. 16, No. 2, April–June 2002

Photochemical and Photothermal Model for Pulsed-Laser Ablation

M. Sadoqi*
St. John's University, Jamaica, New York 11439
S. Kumar†
Polytechnic University, Brooklyn, New York 11201
and
Y. Yamada‡
National Institute of Advanced Industrial Science and Technology, Ibaraki 305-8564, Japan

A model of the interaction of UV laser pulses with organic polymers is presented. The three distinct features of this model are as follows: 1) It combines photochemical and photothermal processes for breaking bonds. 2) It tracks the percentage of bonds broken where the higher dissociative states are not allowed to relax back to the lower states. 3) The model does not need an experimentally inferred value of threshold fluence to determine the onset of ablation. The mathematical model presented here is based on the system of a two-photon absorption model, where sets of rate equations that include radiative transport and energy absorption are solved. Solutions of this model are discussed, and the results are shown to compare well with experimental etch depth vs fluence curves from the literature for a wide range of pulse widths from 7 to 300 ns. Parametric results are also presented for 193- and 308-nm UV laser wavelengths for different laser and polymer parameters. The dependence of the temperatures and ablation depths for different laser fluences and widths of the laser pulses are obtained.

Nomenclature

C_p	=	volumetric specific heat
D	=	thermal diffusivity
F_{th}	=	threshold fluence
h	=	Planck constant
I	=	photon intensity
R	=	electronic to vibrational energy relaxation rate
R_0	=	total number of absorbing chromophores per unit volume
S_0, S_1, S_2	=	chromophore state: ground, first excited, and second excited dissociative
T	=	temperature
α	=	absorption coefficient, $\sigma_1 R_0$
κ	=	Boltzmann constant
ν	=	frequency of laser radiation
ρ_0, ρ_1, ρ_2	=	chromophores per unit volume in states S_0, S_1, and S_2
σ_1, σ_2	=	absorption cross sections of chromophores in states S_0 and S_1
τ	=	relaxation time
τ_p	=	laser pulse width
ω	=	debye frequency

Received 25 June 2001; revision received 20 September 2001; accepted for publication 13 November 2001.

*Assistant Professor, Physics Department, 8000 Utopia Parkway.
†Associate Professor and Othmer Senior Fellow, Mechanical Engineering Department, Six Metrotech Center. Senior Member AIAA.
‡Researcher, Institute for Human Science and Biomedical Engineering, 1-2 Namiki, Tsukuba; also Professor, Department of Mechanical Engineering and Intelligent Systems, University of Electro-Communications, 1-5-1 Chofugaoka, Chofu, Tokyo 182-8585, Japan.

Introduction

THE interaction of UV laser light with organic matters leading to massive material ablation from the target has been investigated for many years.[1–7] Nevertheless, laser ablation is still a growing field in basic science, engineering, and material processing technologies. Despite the large number of scientific and practical applications of the laser-ablation process,[8–14] the basic mechanisms involved are not yet completely understood.

Photoacoustic, reflective, and luminescent emission, as well as high-speed imaging experiments, have been conducted to study the etching process by UV lasers. Through these investigations several important experimental observations have been recorded.[4,15–42] These include the following:

1) Two fluence-dependent parametric regions are observed: a region where negligibly small finite amount of material is removed per pulse and another one where the etch depth increases rapidly with increasing fluence. Based on this observation, the laser ablation process may be characterized to have a threshold fluence above which etching occurs. This experimentally inferred threshold fluence F_{th} is found to correlate with wavelength-dependent absorption coefficient α through the relation $\alpha F_{\text{th}} \sim$ const, based on experimental observations.

2) In addition to fluence, some studies have reported the etch depth to depend on laser pulse width.

3) Thermal effects, such as heating of material and traces of melting/resolidification, are observed in some studies. These have been supported by calorimetric and acoustic measurements in the polymer after it is irradiated with the UV laser.

4) Chemical or physical modification of material after ablation was observed during some experiments.

5) Some experiments report finite removal rates before threshold fluence is reached. Others show that ablation continues after the pulse is removed.

6) Rapid ejection of the molecules and molecular clusters from the target surface resulted in the formation of an expanding plume during the laser ablation process. This was observed through experiments that were specifically instrumented to observe the formation of the plume.

Based on the listed experimental observations and on the chemical/physical properties of polymers, different models of the laser ablation mechanisms have been proposed. These can be categorized as the following:[14,15,19–27,30,38,39]

1) In photochemical models, the breaking of bonds is the direct result of the photon absorption. Here the absorbed photons directly excite the chromophores to higher dissociative states that cause bonds to break.

2) In photothermal models, the bonds are thermally broken. The energy is assumed to be converted into thermal energy described locally by Boltzmann statistics immediately after absorption, and the breaking of bonds is described by an Arrhenius-type rate equation.

Both of the classes of models suffer from drawbacks when applied individually because they alone cannot explain all of the observed phenomena. For example, the photothermal models fail to describe the rapid increase in ablation depth with fluence. In addition, most models developed in the literature, especially photochemical, do not have an intrinsic measure of determining when the etching occurs. Instead they rely on comparing the fluence predicted from the model to the experimentally observed value of threshold fluence to infer if etching has occurred. Another example is that photochemical models cannot predict continuation of ablation after the pulse is removed.

In this paper, a combined photochemical and photothermal model of ablation is developed. The model does not rely on the existence of a known experimental value of threshold fluence to determine the onset of ablation; instead it tracks the number of bonds and their states in the material. When the actual local percentage of bonds that are broken are computed, the material is either considered intact or ablated. This has the advantage of additionally being able to consider materials whose experimental threshold values are not available, or those where a distinct threshold may not be apparent.

Advantages of the previous methods that use the experimentally obtained threshold value are that only absorption of the laser and its related mechanisms of laser–material interaction have to be accounted for. This includes different levels of absorption by various excited states, such as less absorption by higher energy states of the bonds that are created. The other advantage is that only the fluence has to exceed threshold fluence for the material to be considered ablated,[4,22] which leads to a simple modeling framework devoid of the details of the actual etching mechanisms that may be difficult to formulate. The disadvantages are that the actual breaking of bonds and the fragmentation of the material are not accounted for. After the laser pulse is shut off, the model would predict all of the bonds to remain intact and to decay back to the ground state. This would be counterintuitive with etching or fragmentation, where, by definition, a significant percentage of bonds are expected to be irreversibly broken. In addition, some experiments have been reported in the literature where finite removal rates are observed before the threshold fluence is reached. Other experiments also show that ablation continues after the pulse is removed.[24,25] These observations suggest that the concept of threshold fluence is not sacrosanct, and therefore, models based on the existence of such fluence may not be accurate.

The feature and advantage of the present method is that it does not rely on the existence of a known threshold fluence to predict etching, but instead computes the actual percentage of bonds that are broken. However, the disadvantage is that the number of bonds that must be broken for etching to occur is neither experimentally nor theoretically established. The related modeling is also more complicated because of the inclusion of bond breaking mechanisms.

Based on these analyses, the combination of the thermal and chemical models, along with tracking the number of bonds broken, is a very promising method. It gives features of the thermal distribution within the medium and the quantitative and qualitative description of the progress of the etched depth as the medium interacts with the high-intensity laser.

Model Development

Polymers have a broad molecular mass distribution, with a relatively high molecular weight. They are made up of molecules, which consist of 10^3–10^5 atoms, principally carbon, hydrogen, and nitrogen. A small molecular unit (monomer) of 6–40 atoms is repeated over and over along a chain to form a polymer. A polymer may consist of 10^2–10^3 monomer units. The forces between the molecules are weak (10 kcal/mole and 0.43 eV), and the bonding between atoms within a polymer is covalent (shared electrons) in nature and strong (60–185 kcal/mole and 2.6–8.0 eV). Polymers are characterized by high absorption, such as polyimide (PI) and polyethylene terephthalate, or low, such as poly–methylmethacrylate. Photon energies for 193, 248, and 308 nm wavelength lasers are 6.4, 5.0, and 4.0 eV, respectively. When the bond energies are compared with the photon energies, it seems unlikely that absorption of one photon will always cause the breakage of these bonds by means of photochemical reactions.

Given that the mass of an imide monomer is 382 atomic mass units, and the density of PI is 1.43 g/cm^3, the number density of the monomers is 2.3×10^{21} 1/cm^3. The number of absorbed photons per unit volume is characterized by $\alpha F_{th}/h\nu$, which is equal to 4.1×10^{21} 1/cm^3 for 193 nm ($\alpha = 1.5 \times 10^5$ cm^{-1}, $F_{th} = 28$ mJ/cm^2, and 1.75×10^{17} eV/cm^2) and 9.4×10^{21} 1/cm^3 for 308 nm ($\alpha = 0.8 \times 10^5$ cm^{-1}, $F_{th} = 75$ mJ/cm^2, and 4.7×10^{17} eV/cm^2), respectively. Therefore, the number of photons absorbed in one monomer unit of PI at 193 and 308 nm will be approximately 2 and 4, respectively. Each monomer unit has several chromophores and the average based on the numbers of photons and chromophores will yield the value of photons absorbed per chromophore to be less than unity.[20,21,43,44] However, because of the bond strength of the chromophores, two photons will be needed to cause the photochemical breakage of the bonds.

The present model is constructed as follows. The absorbing constituents in the polymer are chromophores of a single type. Initially all chromophores are in the lowest electronic state S_0. All thermal energy associated with the material is present in the vibrational states of S_0. When a chromophore absorbs a photon at the laser frequencies, it is excited to a vibrational state in the upper electronic state S_1. Very rapidly, within a few femtoseconds, the chromophores then relax nonradiatively to the ground vibrational state in S_1. In the model developed in this study, the chromophores at this juncture can either 1) absorb a second photon and be promoted to the upper excited state S_2; 2) relax nonradiatively back to the ground state S_0; 3) relax by emitting a photon, stimulated emission; or 4) be excited to the upper state S_2 by thermal activation. The states and the various transitions considered are shown schematically in Fig. 1. Thermal energy is created mainly by the nonradiative relaxation to the ground state. Small contributions to temperature rise are also due to the relaxation to the ground vibrational state in S_1 or by Stokes shifting where the emitted photon is shifted to a higher wavelength (lower energy) and the remaining energy is thermal in nature. However, these effects are ignored here. Thermal activation from the ground state S_0 to a dissociative state S_2 is neglected in comparison to other activation mechanisms because of corresponding low probability (corresponding to small value of $1/\tau$, see subsequent text for definitions). It is assumed that the state S_2 is a dissociative state and that the bond is broken. Therefore, it cannot relax back to the lower states.

On a qualitative level, absorption of the UV photons by the polymer will excite the materials to upper energy levels. Laser energy will flow throughout the bulk, thereby breaking bonds. Because the typical ablation depth per pulse is a few micrometers or less and the size of the irradiated target is usually at least 100 μm, edge

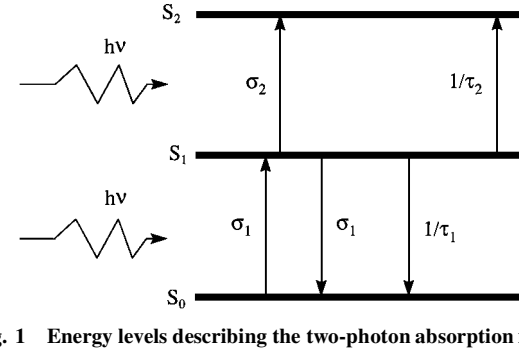

Fig. 1 Energy levels describing the two-photon absorption model.

effect can be neglected, and a one-dimensional model can be used to describe laser pulse propagation into an absorbing medium. The corresponding rate equations are

$$\frac{\partial \rho_0}{\partial t} = \sigma_1(\rho_1 - \rho_0)I + \frac{\rho_1}{\tau_1} \tag{1}$$

$$\frac{\partial \rho_1}{\partial t} = -\sigma_1(\rho_1 - \rho_0)I - \sigma_2\rho_1 I - \frac{\rho_1}{\tau_1} - \frac{\rho_1}{\tau_2} \tag{2}$$

$$\frac{\partial I}{\partial x} = -\sigma_1(\rho_0 - \rho_1)I - \sigma_2\rho_1 I \tag{3}$$

$$C_p\frac{\partial T}{\partial t} = h\nu\frac{\rho_1}{\tau_1} \tag{4}$$

$$R_0 = \rho_0 + \rho_1 + \rho_2 \tag{5}$$

where ρ_0, ρ_1, and ρ_2 and σ_0, σ_1, and σ_2 are the number of chromophores per unit volume (number of chromophores per cubic centimeter) and the effective absorption cross sections (square centimeter per chromophore) in the ground, first excited, and second excited states, respectively. The transition lifetime is denoted by τ. The terms $1/\tau_1$ and $1/\tau_2$ are the transition or relaxation rates (1 over second). The specific heat of the chromophores per unit volume is C_p. The total concentration of absorbing chromophores per unit volume is R_0 (chromophores per cubic centimeter), which is constant and is equal to the number of chromophores ρ_0 in the ground state S_0 before the laser is incident. The term $1/\tau_2$ is based on the assumption that the transition from the first excited to the second excited state by thermal activation is approximately Boltzman, that is,

$$1/\tau_2 = \omega \exp(-E_{\text{act}}/\kappa T) \tag{6}$$

where E_{act} is the activation energy. The intensity I is a photon flux (photons per second per square centimeter). Note that the pulse intensity, temperature, and chromophore population numbers depend on time and position, that is, $I = I\ (x, t)$, $T = T\ (x, t)$, and $\rho_i = \rho_i(x, t)$. The absorption cross sections are strong functions of incident wavelength, $\sigma = \sigma(\lambda)$ The characteristic time for heating is long compared to the electronic relaxation time, which is on the order of picoseconds and less, but is much shorter than the laser pulse duration,[44] which is in the range of nanoseconds. However, the characteristic time it takes for heat to be redistributed down to depths of the order of the radiation penetration depth $1/\alpha$ is much longer than the pulse duration:

$$1/R \ll \tau_p \ll 1/2\alpha^2 D \tag{7}$$

Heat conduction during the laser pulse is neglected. This can be justified by Eq. (7) where the thermal diffusivity D is in square centimeters per second. For the PI, the value of D is 4×10^{-4} cm^2/s.

Equation (1) indicates that the rate of increase of chromophores in the S_0 state is due to the radiative and nonradiative relaxations from S_1 state and that the decrease is caused by the excitation from S_0 to S_1 via absorption of laser energy. The rate of increase of S_1 state chromophores is caused by the excitation from S_0, and the decrease is due to the radiative and nonradiative relaxations and decay to S_0 and excitation to S_2 states via photon absorption and thermal activation, respectively [Eq. (2)].

Once the chromophores reach the S_2 state, they are assumed to be dissociated. This is different from all of the other models in the literature where relaxation from S_2 state to the lower states is permitted. In the present model, therefore, the energy transferred to the S_2 state is carried away from the bulk material, and the ablated chromophores no longer participate in the rate equations.

Equation (3) evaluates the rate of spatial change of intensity by considering the attenuation due to absorption by the chromophores in the ground and first excited states as they are excited to the first and second excited states, respectively, and the emission by the radiative relaxation from the first state to the ground state.

The right-hand side of Eq. (4) is the energy deposition rate in the bulk material, where C_p is the specific heat in joules per cubic centimeter per Kelvin. The left-hand side of Eq. (4) is the heat deposition rate to the material. The dominant mechanism of the heating in the sample is nonradiative transitions. A nonradiative transition between electronic states transfers the electronic energy to vibrational, rotational, and transitional modes of the material, temporarily imparting a very high effective temperature. The effective temperature is the energy equivalent temperature. Other thermal analyses in the literature have shown such energy equivalent temperatures to be several thousand Kelvin (Ref. 42). As specified by Eq. (7), the heat conduction mechanisms are not included in Eq. (4), and the present model as described by Eq. (4) only considers the dominant heating mechanism.

The features of the model presented in Eqs. (1–5) are as follows. 1) The model considers simultaneously the photochemical and photothermal effects. 2) Thermal energy is generated by the nonradiative relaxation from the excited to the ground state. 3) The highest state is dissociative, and chromophores cannot relax back to lower states once they reach this level. 4) The combined model can predict a continuation of the etching process via retained thermal energy even after the pulse is shut off. 5) The model can also predict etching by thermal and other mechanisms before the threshold fluence is reached.

The advantages of the current model over existing ones are numerous. First, it considers the effects of photochemical and photothermal mechanisms simultaneously. This permits many observed effects to be included such as continuation of ablation after the pulse has ended. Second, ablation in the model is considered to occur only when a bond reaches a dissociative state and is, therefore, broken. Such bonds cannot subsequently relax back to ground state, and this feature rectifies the drawback that is present in many existing formulations. Finally, the model can use either threshold fluence as a marker for etching or percentage of bonds broken with equal ease. It can, therefore, also be used to compare the two methods of determining when the etching has occurred.

Results

We now present the results of our study of the laser ablation of organic materials. An analysis of the microscopic mechanisms of laser ablation is combined with an investigation of the interaction between the different parameters of the ablation process. The temperature effects on the depth of ablation for different laser parameters such as pulse width and energy are also investigated. The material properties used here to perform the numerical simulations are presented in Table 1. These are taken from the literature to represent typical values. The thermal activation energy E_{act} is taken to be the carbon–carbon single-bond strength.[38,42,43]

The coupled equations that model the number density of chromophore states, the intensity, and the temperature in the medium [Eqs. (1–6), are solved by a finite difference scheme that is explicit in time. Grid sizes and time steps are selected to ensure that numerical results are independent of spatial and temporal increments. The experimental values that are used to validate the numerical results of

Table 1 Parameters used for calculation[38,42,43]

Parameter[a]	Values
R_0, cm^{-3},	
At 193 nm	1.82×10^{22}
At 308 nm	8.0×10^{22}
C_p, J/K · cm^3	1.55
α, cm^{-1}	
At 193 nm	2.8×10^5
At 308 nm	0.8×10^5
σ_1, cm^2	
At 193 nm	1.55×10^{-17}
At 308 nm	1.0×10^{-18}
E_{act}, kJ/mol	502
F_{th}, J/cm^2	
At 193 nm	0.03
At 308 nm	0.07
ω, s^{-1}	1.0×10^{13}

[a]Here, σ_2 was taken as $\sigma_1/2$, τ_1 was taken as 35 ps.

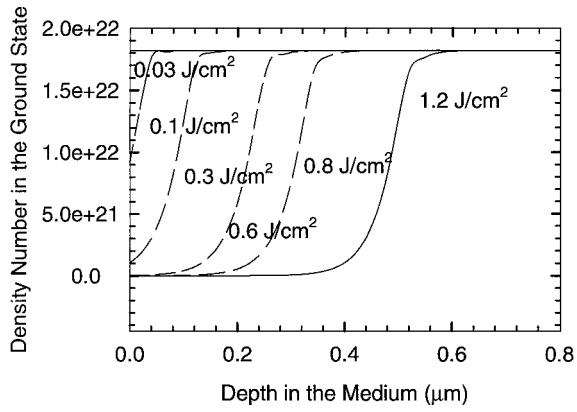

Fig. 2a Density number of PI in ground state at end of the pulse after irradiation by 193-nm UV laser wavelength of 7-ns pulse width for different fluences, $F_{th} = 0.03$ J/cm^2.

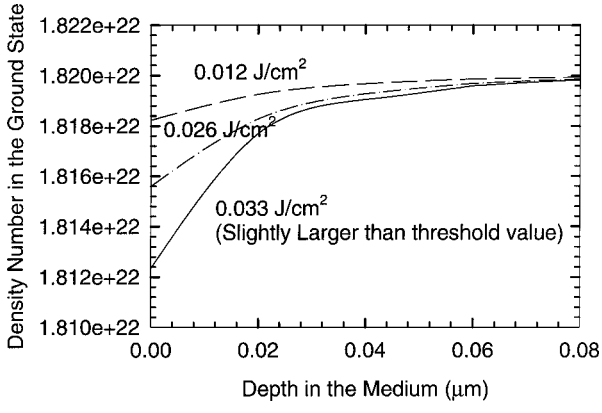

Fig. 2b Density number of PI in ground state at end of the pulse after irradiation by 193-nm UV laser wavelength of 7-ns pulse width for different fluences below the threshold fluence, $F_{th} = 0.03$ J/cm^2.

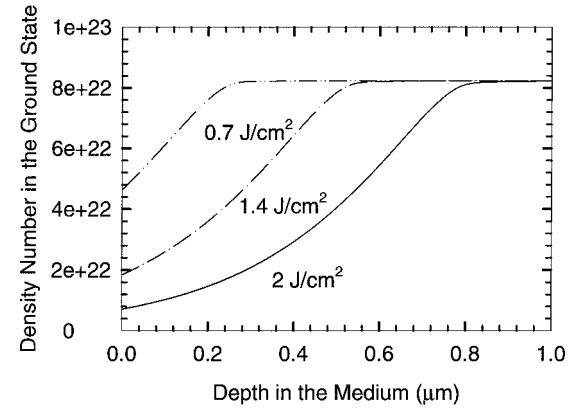

Fig. 3a Density number of PI in ground state at the end of the pulse after irradiation by 308-nm UV laser wavelength of 7-ns pulse width for different fluences, $F_{th} = 0.07$ J/cm^2.

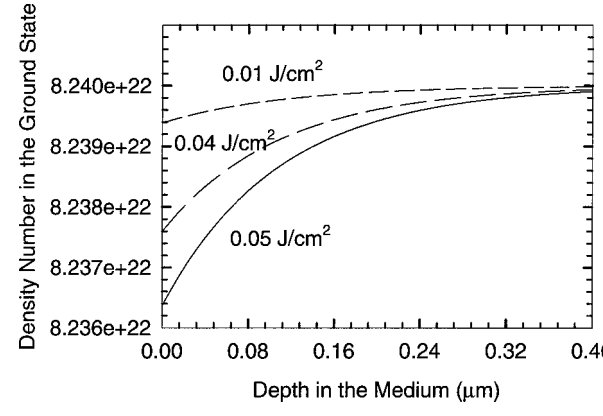

Fig. 3b Density number of PI in ground state at end of the pulse after irradiation by 308-nm UV laser wavelength of 7-ns pulse width for different fluences below the threshold fluence, $F_{th} = 0.07$ J/cm^2.

the model are obtained from the literature. The experimental uncertainty has not been discussed in these references, and therefore, no estimate of experimental uncertainty is presented in the present study.

We start from the analysis of the variation of the density number in the ground state with depth of the medium for different fluence as shown in Figs. 2 and 3. We considered two different laser wavelengths, 193 and 308 nm, at the same pulse width 7 ns, and the threshold fluences were 0.03 and 0.07 J/cm^2, respectively, as reported in the literature. A mere visual inspection of the plots shows an apparent similarity in the evolution of the density number in the ground state inside the target as we vary the laser fluence. Both cases show the number of intact bonds in the ground state is very small near the surface and 100% in the unetched virgin material. As the fluence becomes higher, more of the material is affected, and bonds are broken deeper into the material. As the intensity increases, we begin to observe a nonlinear profile of the chromophore number density being formed. This profile moves into the medium as the intensity increases. The plots of the lower fluences, as shown in Figs. 2b and 3b, respectively, indicate that the etching process starts below threshold fluence as observed in some experimental studies.[4,21] As shown in Figs. 2 and 3, at 193 nm the area of the material that is excited to the higher states is smaller than that at 308 nm, and therefore, the etching depth is consistently smaller.

When the number of chromophores in the first excited state is also examined (Figs. 4 and 5), it can be inferred that a very small percentage of the chromophores remain in the first excited state. The reason that the excited state chromophores are so few in number is that the relaxation processes from the first excited state are quite rapid compared to the other mechanisms in the process. When the numbers of chromophores in the ground and first excited states are compared to the total number of chromophores, it is seen that near

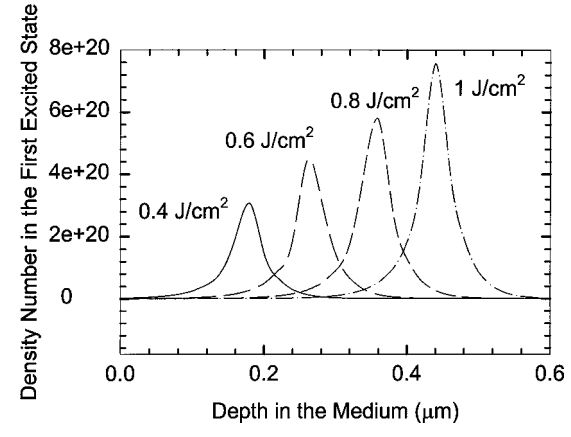

Fig. 4 Density number of PI in first excited state at the end of pulse after irradiation by 193-nm UV laser wavelength of 7-ns pulse width for different fluences.

the surface of the polymer most of the chromophores are in the dissociative second excited state where the bonds are broken.

The results shown in Figs. 2–5 can be used to compare with the fluence values inside the medium. If the location at which the local fluence is equal to the threshold fluence value obtained from the literature is taken to be the etch depth, Fig. 6 can be constructed from the model. When the number density of the chromophores at these depths is examined, the following significant conclusion can be drawn. It is seen that at the etch depth obtained by considering the location at which fluence equals threshold fluence the number of intact bonds in the ground state is approximately 90%. Between the surface and this etch depth location, the number of intact ground

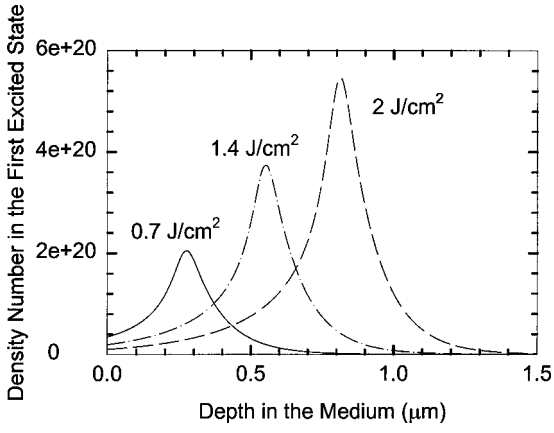

Fig. 5 Density number of PI in first excited state at the end of pulse after irradiation by 308-nm UV laser wavelength of 7-ns pulse width for different fluences.

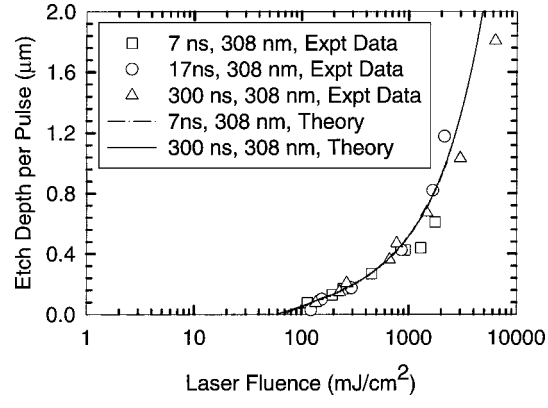

Fig. 6 Comparison of theoretical etch depth per pulse (solid lines) vs log fluence with experimental data (open symbols) for etching PI by a 308-nm UV laser of 7-, 17-, and 300-ns pulse widths.

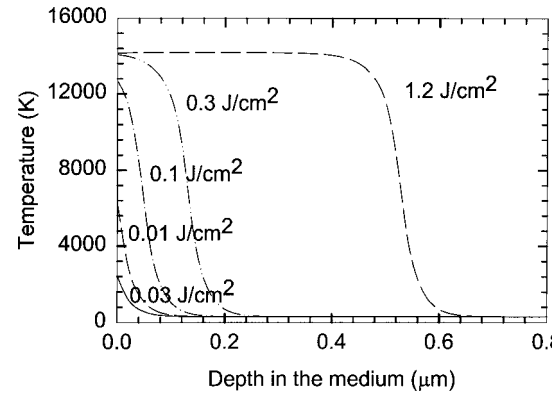

Fig. 7 Distribution of temperature within PI at 7 ns after irradiation by 193-nm UV laser wavelength of 7-ns pulse width for different fluences.

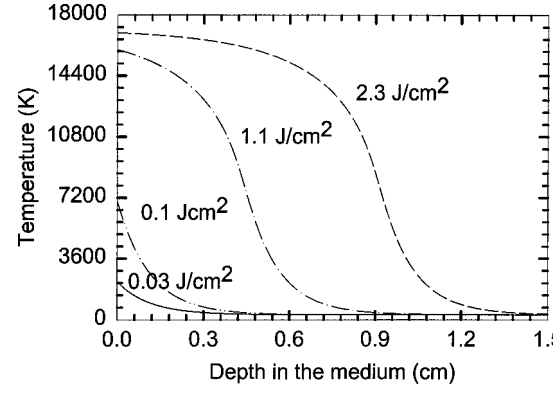

Fig. 8 Distribution of temperature within PI at 7 ns after irradiation by 308-nm UV laser wavelength of 7-ns pulse width for different fluences.

state chromophores is less that 90%, and the virgin material has more than 90% intact ground state bonds. In other words, 10% or more of original ground state bonds have to vanish for the region to be considered ablated. If the number of intact bonds at a lower percentage, for example, 50%, are considered to mark the etch depth, the corresponding difference will be small for 193 nm but larger for 308 nm. However, the trends of etch depth vs fluence will remain the same. Thus, whereas the exact number may differ, the trends presented by considering either the threshold fluence or the percentage of bonds broken are similar and are, therefore, equally valid.

Figure 6 also shows the accuracy of the present model by comparing with experimental values.[32,43] The match between experimental results and predictions instills confidence in the model and its results. The experimental results from the references cited are based on collection of data from the literature. No experimental error estimates have been provided and are, therefore, not reported here.

Figures 7 and 8 show the temperature as a function of depth of the medium for different laser fluences for 193 and 308 nm wavelengths at 7 ns width of laser pulse. Figures 7 and 8 give a quantitative analysis of the distribution of the temperature inside the medium. For laser fluence below threshold fluences, the temperature attenuates into the medium, and the surface temperature increases as laser fluences increase. However, as the fluence increases, we observe different behavior of the temperature distribution inside of the medium. This includes the following. 1) The rate of temperature rise at the surface with increasing fluence decreases as the fluence value becomes larger. 2) The slope of temperature in the medium at the surface decreases as fluence rises, and as we continue to increase fluence, the slope becomes zero. 3) The attenuating temperature profile proceeds deeper inside of the medium with increasing fluence. Because temperature depends on the value of the energy absorbed locally (conduction is not included), the temperature stabilizes after the chromophores have reached the highest excited dissociative state and cannot relax back to lower states. At this juncture, there is no nonradiative relaxation to provide the energy for absorption and for the corresponding temperature rise. Additionally, as the medium saturates, that is, more bonds are in the higher states that are less absorptive, less energy is absorbed, and the heating decreases.

The values of temperature rise are high, especially near the surface. The temperatures are the energy equivalent temperatures, and actual temperatures are expected to be lower if other modes of energy transport and absorption were considered, such as conduction, plume generation, polymer melting/decomposition, acceleration of decomposing products in the plume, and others. Surface temperature rises in excess of 10,000 K are reported in an analytical study.[42] Another study has estimated surface temperatures to rise by about 850 K at their selected values of threshold fluence (0.014 and 0.037 J/cm^2 for 193 and 308 nm wavelengths, respectively).[44] The temperature values computed in this study are of the same order if these published results are extrapolated to the fluences considered in the present study.

Figures 9 and 10 present the surface temperature vs incident fluence for different pulse durations. For fluence below the threshold fluence, the temperature at the surface of the target is linear with the fluence for three different width pulses as shown here, 7, 17, and 300 ns. The pulse width is seen to have a negligible influence on the temperature. The surface temperature reaches a plateau as fluence increases beyond the threshold values because the all of the chromophores near the surface are at the highest dissociative state and thus cannot relax back, thereby eliminating the source of energy for the temperature rise. In models, such as those presented in the literature, where the chromophores at the highest excited state are allowed to relax to lower states, the surface temperature would continue to increase with fluence. Further research is also needed

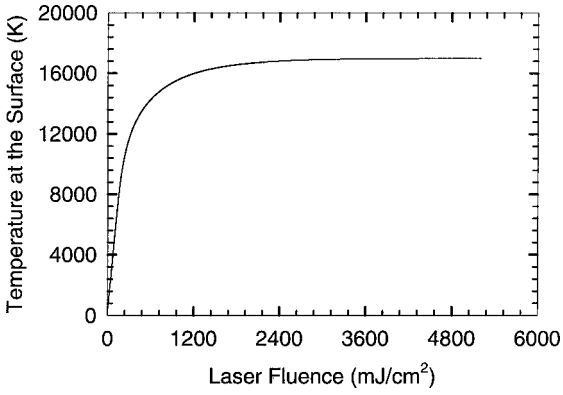

Fig. 9 Surface temperature vs laser fluence for different durations of the pulse of PI after irradiation by 308-nm UV laser wavelength.

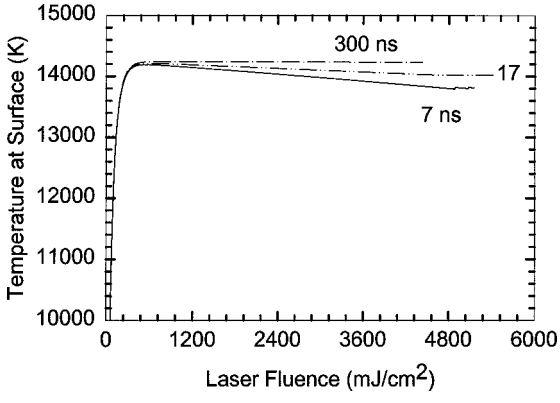

Fig. 10 Surface temperature vs laser fluence for different durations of pulse of PI after irradiation by 193-nm UV laser wavelength.

to study the effects of plume formation[45] and the effect of multiple pulses.[46]

Conclusions

The paper presents a comprehensive model that includes photochemical and photothermal mechanisms of ablation. Dissociative excited states are considered that cannot relax back to lower states. Thus, the model can track the number of bonds that are broken.

Etch depth can be evaluated by considering the location in the material at which the fluence reaches the threshold fluence, as is traditionally done, or by examining the fraction of chromophores that are in the highest dissociative state, as is feasible by the current method. The results show that both of these yield etch depths that follow the same trends, though they may differ in values. The results of the study indicate that, for the cases examined, the etch depths predicted by the two definitions are the same if either the threshold fluence is the marker for the onset of ablation or if more that 10% of the ground state chromophores have transitioned to the highest dissociative state. That is, the material can be considered etched if the number of intact bonds falls below 90%, or if more that 10% of the chromophores are in the highest dissociative state. Further research that considers several other cases will be needed to identify a universally acceptable percentage value.

Acknowledgments

Part of this work was supported by the Science and Technology Agency fellowship program of the Japanese government. Discussions with Peter Riseborough of Temple University are also acknowledged.

References

[1]Kawamura, Y., Toyoda, K., and Namba, S., "Effective Deep Ultraviolet Photoetching of Polymethylmethacrylate by an Excimer Laser," *Applied Physics Letters*, Vol. 40, No. 5, 1982, pp. 374, 375.

[2]Srinivasan, R., and Leigh, W. J., "Ablative Photodecomposition: Action of Far-Ultraviolet (193nm) Laser Radiation on Poly(ethylene-terephthalate) Films," *Journal of the American Chemical Society*, Vol. 104, No. 24, 1982, pp. 6784, 6785.

[3]Srinivasan, R., and Mayne-Banton, V., "Self-Developing Photoetching of Poly(ethylene terephthalate) Films by Far-Ultraviolet Excimer Laser Radiation," *Applied Physics Letters*, Vol. 41, No. 6, 1982, pp. 576–578.

[4]Andrew, J. E., Dyer, P. E., Forster, D., and Key, P. H., "Direct Etching of Polymeric Materials Using a XeCl Laser," *Applied Physics Letters*, Vol. 43, No. 8, 1983, pp. 717–719.

[5]Geis, M. E., Randall, J. N., Deutsch, T. F., Degraff, P. D., Krohn, K. E., and Stern, L. A., "Self-Developing Resist with Submicrometer Resolution and Processing Stability," *Applied Physics Letters*, Vol. 43, No. 1, 1983, pp. 74–76.

[6]Deutsch, T. F., and Geis, M. W., "Self-Developing UV Photoresist Using Excimer Laser Exposure," *Journal of Applied Physics*, Vol. 54, No. 12, 1983, pp. 7201–7204.

[7]Rice, S., and Jain, K., "Direct High Resolution Excimer Laser Photoetching," *Applied Physics A*, Vol. 33, No. 3, 1984, pp. 195–198.

[8]Levis, R. J., "Laser Desorption and Ejection of Biomolecules from Condensed Phase into Gas Phase," *Annual Review of Physical Chemistry*, Vol. 45, 1994, pp. 483–518.

[9]Jacques, S. L. (ed.), *Laser-Tissue Interaction IX*, SPIE Proceedings Series, Vol. 3254, Society of Photo-Optical Engineers, Washington DC, 1998.

[10]Miller, J. C., and Haglund, R. F., Jr. (eds.), *Laser Ablation and Desorption*, Academic Press, London, 1998.

[11]Srinivasan, R., and Braren, B., "Ultraviolet Laser Ablation and Etching of Polymethyl-Methacrylate Sensitized with an Organic Dopant," *Applied Physics A*, Vol. 45, No. 4, 1988, pp. 289–292.

[12]Metev, S. M., and Veiko, V. P., *Laser-Assisted Microtechnology*, Springer, Berlin, 1998.

[13]Chrisey, D. B., and Hubler, G. K., (eds.), *Pulsed Laser Deposition of Thin Films*, Wiley, New York, 1994.

[14]Paine, C. D., and Bravmen, J. C., (eds.), *Laser Ablation for Materials Synthesis*, Materials Research Society, Pittsburgh, PA, 1990.

[15]Jellinek, H. H. G., and Srinivasan, R., "Theory of Etching of Polymers by Far-Ultraviolet, High-Intensity Pulsed Laser and Long Term Irradiation," *Journal of Physical Chemistry*, Vol. 88, No. 14, 1984, pp. 3048–3051.

[16]Koren, G., and Yeh, J. T. C., "Emission Spectra, Surface Quality, and Mechanism of Excimer Laser Radiation," *Applied Physics Letters*, Vol. 44, No. 12, 1984, pp. 1112–1114.

[17]Dyer, P. E., and Sidhu, J., "Excimer Laser Ablation and Thermal Coupling Efficiency to Polymer Films," *Journal of Applied Physics*, Vol. 57, No. 4, 1985, pp. 1420–1422.

[18]Gorodetsky, G., Kazyaka, T. G., Melcher, R. L., and Srinivasan, R., "Calometric and Acoustic Study of Ultraviolet Laser Ablation of Polymers," *Applied Physics Letters*, Vol. 46, No. 9, 1985, pp. 828–830.

[19]Srinivasan, V., Smrtic, M. A., and Babu, S. V., "Excimer Laser Etching of Polymers," *Journal of Applied Physics*, Vol. 59, No. 11, 1986, pp. 3861–3867.

[20]Brannon, J. H., Lankard, J. L., Baise, A. I., Burns, F., and Kaufman, J., "Excimer Laser Etching of Polyimide," *Journal of Applied Physics*, Vol. 58, No. 5, 1985, pp. 2036–2048.

[21]Srinivasan, R., and Braren, B., "Ablative Photodecomposition of Polymer Films by Pulsed Far-Ultraviolet (193nm) Laser Radiation: Dependence of Etch Depth on Experimental Conditions," *Journal of Polymer Science*, Vol. 22, No. 10, 1984, pp. 2601–2609.

[22]Srinivasan, R., Braren, B., and Dreyfus, R., "Ultraviolet Laser Ablation of Polyimide Films," *Journal of Applied Physics*, Vol. 61, No. 1, 1987, pp. 372–376.

[23]Dyer, P. E., and Srinivasan, R., "Nanosecond Photoacoustic Studies on Ultraviolet Laser Ablation of Organic Polymers," *Applied Physics Letters*, Vol. 48, No. 6, 1986, pp. 445–447.

[24]Garrison, B. J., and Srinivasan, R., "Microscopic Model for the Ablative Photodecomposition of Polymers by Far-Ultraviolet Radiation (193 nm)," *Applied Physics Letters*, Vol. 44, No. 9, 1984, pp. 849–851.

[25]Garrison, B. J., and Srinivasan, R., "Laser Ablation of Organic Polymers: Microscopic Models for Photochemical and Thermal Processes," *Journal of Applied Physics*, Vol. 57, No. 8, 1985, pp. 2909–2914.

[26]Chuang, M. C., and Tam, A. C., "On the Saturation Effect in the Picosecond Near Ultraviolet Laser Ablation of Polyimide," *Journal of Applied Physics*, Vol. 65, 1989, pp. 2591–2595.

[27]Simon, P., "Time Resolved Ablation Site Photography of XeCl Laser Irradiated Polyimide," *Applied Physics B*, Vol. 48, No. 3, 1989, pp. 253–256.

[28]Keyes, T., Clarke, R. H., and Isner, J. M., "Theory of Photoablation and its Implications for Laser Phototherapy," *Journal of Physical Chemistry*, Vol. 89, 1985, pp. 4194–4196.

[29]Paetzel, R., Stamm, U., Bragin, I., Voss, F., Nikolaus, B., Endert, H., and Basting, D., "Excimer Lasers for Material Ablation Cross the 1.5 kHz Mark," *SPIE Proceedings*, Vol. 2992, 1997, pp. 2–6.

[30]Sutcliffe, E., and Srinivasan, R., "Dynamics of UV Laser Ablation of Organic Polymer Surfaces," *Journal of Applied Physics*, Vol. 60, No. 9, 1986, pp. 3315–3322.

[31]Kuper, S., and Stuke, M., "Femtosecond UV Excimer Laser Ablation," *Applied Physics B*, Vol. 44, No. 4, 1987, pp. 199–204.

[32]Taylor, R. S., Singleton, D. L., and Paraskevopoulos, G., "Effect of the Optical Pulse Duration on the XeCl Laser Ablation of Polymers and Biological Tissues," *Applied Physics Letters*, Vol. 50, No. 25, 1987, pp. 1779–1781.

[33]Kim, H., Postlewaite, J. C., Zyung, T., and Dlott, D. D., "Time Dependent Self Focusing and 20 ps Delay in Laser Ablation of Polymers," *Applied Physics Letters*, Vol. 54, No. 22, 1989, pp. 2274–2276.

[34]Klopotek, P., Burghardt, B., Muckenheim, W., "Short Pulses from Excimer Lasers," *Journal of Physics E*, Vol. 20, No. 10, 1987, pp. 1269, 1270.

[35]Pettit, G. H., and Sauerbrey, R., "Fluence-Dependent Transmission of Polyimide at 248 nm Under Laser Ablations Conditions," *Applied Physics Letters*, Vol. 58, No. 8, 1991, pp. 793–795.

[36]Lazare, S., and Granier, V., "Empirical Photoablation Rate Model Exemplified with the Etching of Polyphenylquinoxaline," *Applied Physics Letters*, Vol. 54, No. 9, 1989, pp. 862–864.

[37]Furzikof, N. P., "Approximate Theory of Highly Absorbing Polymer Ablation by Nanosecond Laser Pulses," *Applied Physics Letters*, Vol. 56, No. 17, 1990, pp. 1638–1640.

[38]Cain, S. R., Burns, F. C., Otis, C. E., and Braren, B., "Photothermal Description of Polymer Ablation: Absorption Behavior and Degradation Time Scales," *Journal of Applied Physics*, Vol. 72, No. 11, 1992, pp. 5172–5178.

[39]Palmer, B. J., Keyes, T., Clarke, R. H., and Isner, J. M., "Theoretical Study of Ablative Photodecomposition in Polymeric Solids," *Journal of Physical Chemistry*, Vol. 93, No. 21, 1989, pp. 7509–7516.

[40]Cain, S. R., Burns, F. C., and Otis, C. E., "On Single-Photon Ultraviolet Ablation of Polyimide Materials," *Journal of Applied Physics*, Vol. 71, No. 9, 1992, pp. 4107–4117.

[41]Pettit, G. H., and Sauerbrey, R., "Theory for the Etching of Organic Materials by Ultraviolet Laser Pulses," *Applied Physics Letters*, Vol. 55, No. 5, 1989, pp. 421–423.

[42]Cain, S. R., "A Photothermal Model for Polymer Ablation: Chemical Modification," *Journal of Physical Chemistry*, Vol. 97, No. 29, 1993, pp. 7572–7577.

[43]Pettit, G. H., and Sauerbrey, R., "Pulsed Ultraviolet Laser Ablation," *Applied Physics A*, Vol. 56, No. 5, 1993, pp. 51–63.

[44]Kuper, S., Brannon, J., and Brannon, K., "Threshold Behavior in Polyimide Photoablation: Single-Shot Rate Measurements and Surface-Temperature Modeling," *Applied Physics A*, Vol. 56, No. 1, 1993, pp. 43–50.

[45]Domen, K., and Chuang, T. J., "Laser Induced Photodissociation and Desorption," *Journal of Chemical Physics*, Vol. 90, No. 6, 1989, pp. 3332–3338.

[46]George, S., and Mitra, K., "Analysis of Ablation Characteristics of Absorbing Dielectrics Caused by Short Laser Pulses," *Journal of Thermophysics and Heat Transfer*, Vol. 15, No. 2, 2001, pp. 190–196.